



Published in final edited form as:

J Vasc Surg. 2010 April ; 51(4): 951–961. doi:10.1016/j.jvs.2009.11.075.

Loss of STAT1 is Associated with Increased Aortic Rupture in an Experimental Model of Aortic Dissection and Aneurysm Formation

Matthew J. Eagleton, MD^{*,1,2}, Jun Xu, BS¹, Mingfang Liao, MD³, Brittney Parine, BS¹, Guy M. Chisolm, PhD², and Linda M. Graham, MD^{1,2}

¹Department of Vascular Surgery, Cleveland Clinic Foundation, Cleveland, OH

²Department of Biomedical Engineering, Cleveland Clinic Foundation, Cleveland, OH

Department of Vascular Surgery, Changhai Hospital, Secondary Military Medical University, Shanghai, PR China

Abstract

Background—Transcription factor signal transducer and activator of transcription (STAT) 1 has been linked to a variety of pathologic states involved with matrix remodeling, but its role in aortic pathology has not been previously described. The current study hypothesizes that STAT1 regulates aneurysmal degeneration and its role will be evaluated in human aortic aneurysms and in a mouse model of aortic dissection.

Methods—Apolipoprotein E knockout mice (ApoE^{-/-}) or ApoE/STAT1 double knockout mice (ApoE/STAT1^{-/-}) were infused with 1000 ng/kg/min of angiotensin II (Ang II). Systolic blood pressure (SBP) was measured in the rodent tail. At sacrifice, aortic diameters and extent of aneurysm formation were measured by digital microscopy. STAT1 and phosphorylated-STAT1 protein levels were assessed in ApoE^{-/-} mice at 0, 7, 14, and 28 days (n=8/time point) by ELISA. Histology was performed using H&E and Movat stains. Statistical analyses included chi-square test, T-test, and ANOVA.

Results—STAT1 mRNA and total protein were greater in human AAA compared to non-aneurysmal controls. In addition, aneurysms occurred in 8%, 50%, and 80% of apoE^{-/-} mice at 7, 14, and 28 days respectively. Total STAT1 levels were not altered during the course of Ang II infusion, but phosphorylated STAT1 levels peaked at 7 days with a 1.4-fold increase over baseline (P<0.05). Aneurysms occurred in 0%, 100%, and 100% of apoE/STAT1^{-/-} mice at 3, 5, and 28 days. In mice infused with Ang II for more than 3 days, aortic rupture occurred more frequently in apoE/STAT^{-/-} mice (53% v. 19%, P<0.05) and at earlier time points (4.0±0.5 v. 9.2±0.77 days, P<0.05) compared with apoE^{-/-} mice. SBP did not differ between the groups during Ang II infusion. By 28 days, aneurysms were larger in apoE/STAT1^{-/-} mice compared to apoE^{-/-} mice (2.7±0.4 v. 1.9±0.1 mm, P<0.05), and were more extensive arising at the level of the left subclavian artery and extending to the infrarenal aorta. H&E and Movat stain did not reveal differences in aortic wall

© 2009 The Society for Vascular Surgery. Published by Mosby, Inc. All rights reserved.

*To Whom Correspondence Should be Addressed: Matthew J. Eagleton, MD, Department of Vascular Surgery, H32, Cleveland Clinic Foundation, 9500 Euclid Avenue, Cleveland, OH 44195. Office: 216-445-1167, Fax: 216-444-9324, eagletm@ccf.org.

Publisher's Disclaimer: This is a PDF file of an unedited manuscript that has been accepted for publication. As a service to our customers we are providing this early version of the manuscript. The manuscript will undergo copyediting, typesetting, and review of the resulting proof before it is published in its final citable form. Please note that during the production process errors may be discovered which could affect the content, and all legal disclaimers that apply to the journal pertain.

Presented before the Vascular Annual Meeting, June 12, 2009, Denver, OH

structural content at baseline between apoE^{-/-} and apoE/STAT1^{-/-} mice, and both groups demonstrated equal disorganization in the aneurysmal state.

Conclusions—Phosphorylated STAT1 is elevated during aneurysmal degeneration and its loss is associated with a higher rate of acute aortic rupture and more extensive aneurysms in a mouse model of aortic dissection. Further investigation is necessary to determine whether these observations are secondary to an underlying aortic wall abnormality, or alterations in vessel wall matrix remodeling.

Abdominal aortic aneurysm (AAA) formation is a multifactorial process resulting from the altered homeostasis of aortic wall matrix protein production and destruction. Multiple mechanisms contribute to the development of aneurysms. One endpoint of these mechanisms is the upregulation of enzymes capable of degrading the extracellular matrix (ECM) structural proteins. The production of new matrix proteins by aortic smooth muscle cells (SMC) is insufficient to compensate for this, resulting in weakening of the aortic wall. Pivotal enzymes involved in this process include matrix metalloproteinases (MMPs), plasminogen activators, and serine elastases 1-3. While these enzymes are clearly important in aneurysm formation, there is a growing body of evidence demonstrating the significance of the proteins involved in regulating their expression. Inhibition of c-Jun N-terminal kinase, a mitogen-activated protein kinase, not only prevents experimental AAA formation, it may cause regression of the aneurysms⁴. In addition, inhibition of transcription factors nuclear factor (NF)- κ B and ets ameliorate AAA formation in an experimental animal model⁵. In fact, the combined inhibition of both of these transcription factors has led to the regression of experimental AAA formation⁴.

STAT proteins are a family of transcription factors that exist as inactive monomers, which are phosphorylated, form homo- or hetero-dimers, and translocate to the nucleus. The classic model for STAT activation depends on a series of tyrosine phosphorylations that are carried out by JAK proteins, a family of membrane receptor-associated tyrosine kinases⁶. Phosphorylated STATs dimerize, translocate to the nucleus, and bind to specific gene activation sites resulting in induction, or inhibition, of transcription of downstream target genes⁷. Seven different STAT family members have been characterized (STAT-1, -2, -3, -4, -5 α , -5 β , -6), and have been associated with numerous cytokine, growth factor, and interferon receptors. In normal cells, the activation of STAT proteins is transient, ranging from a few minutes to a few hours. In disease states, however, constitutive activation of STATs can occur⁸.

STAT1 is a ubiquitous transcription factor that has, classically, been associated with IFN γ signaling, although other triggers of its activation have been deemed equally important. STAT1 is activated by phosphorylation of tyrosine 701. Alternatively, STAT1 may be phosphorylated by serine 727 phosphorylation. Tyrosine and serine phosphorylation are not interdependent, and STAT1 can be selectively phosphorylated on tyrosine residues, serine residues, or both. In addition, STAT1 may form a homodimer, or a heterodimer with phosphorylated STAT2 or STAT3. The site of phosphorylation, the dimers subsequently formed, and the cell/tissue location determine the downstream specificity of STAT1. Its activation has been associated with regulation of apoptosis and extracellular matrix regulation, both processes that have are important to aneurysm formation⁶. While recently STAT1 has been implicated in atherogenesis, its role in aneurysm formation has not previously been reported⁹.

This current study hypothesizes that STAT1 is important in aortic aneurysm formation. This study will evaluate the expression of STAT1 in human AAA and an experimental model of aneurysm formation, and it will evaluate the significance of this transcription factor in experimental aneurysm development.

Methods

Apolipoprotein E knockout mice (ApoE null mice) were originally obtained from the Jackson Laboratory (Bar Harbor, ME), while apolipoprotein E/STAT1 double knockout mice (ApoE/STAT1 null mice) were a generous gift from Dr. Chisolm⁹. Both strains were maintained in breeding colonies in the Lerner Research Institute at the Cleveland Clinic. All experiments and procedures were approved by the Cleveland Clinic IACUC (protocol approval number). All reagents, unless otherwise stated, were obtained from Sigma (St. Louis, MO).

Aortic Aneurysm

Human aortic aneurysm tissue was obtained from patients undergoing surgery for an abdominal aortic aneurysm (N=12), while control aortic tissue was obtained from patients during organ procurement (N=9), snap frozen in liquid nitrogen, and stored at -80°C until further use. Limited demographic data are available on the “normal” aortic samples and are limited to age, gender, and race. ApoE null mice (N=95), STAT1 null mice (20), and apoE/STAT1 null mice (N=56), 3–6 months of age, of male gender, and on normal chow diets had subcutaneous osmotic minipumps (Model 2004, ALZA Scientific Products, Mountain View, CA) implanted under ketamine (150 mg/kg) and xylazine (7.5 mg/kg) anesthesia. Pumps were filled with sufficient concentration of angiotensin II (Ang II) to provide a continuous infusion of 1000 ng/kg/min of Ang II for up to 28 days. Mice were sacrificed at 0, 3, 5, 7, 14, and 28 days (n=8/strain/time point) of Ang II infusion. In addition, male STAT1 null mice (N=20) (Taconic, Hudson, NY), female apoE null mice (N=10), and female apoE/STAT1 null mice (N=10) underwent infusion of Ang II for a total of 28 days prior to sacrifice. Prior to sacrifice, maximum aortic diameter was measured using a micrometer. The micrometer was normalized to a known length (ruler) prior to each measurement. In addition, aortic morphology was assessed and assigned to one of the following categories: normal, type I (dilated lumen, no thrombus), type II (remodeled tissue with intraluminal thrombus), type III (bulbous form of type II), and type IV (multiple, diffuse aneurysm with intraluminal thrombus) as has previously been described¹⁰. Aneurysms were considered present if the diameter was 100% greater than corresponding aortic segments of mice not infused with Ang II.

Indirect systolic blood pressure (SBP) measurement

Systolic blood pressures were obtained in unanesthetized mice prior to pump implantation and again during Ang II infusion. Mice were acclimated to the restrainer (IITC Life Sciences, Woodland Hills, CA) and warming chamber (kept at $31\text{--}34^{\circ}\text{C}$) for two days prior to these measurements. Pressure measurements were obtained through an integrated tail sensor-cuff occluder, and readings taken over the course of 10 minutes as previously described¹¹.

Quantitative (real-time) reverse transcriptase-polymerase chain reaction (RT-PCR)

Expression of mRNA levels of ribosomal 18S-rRNA (Hs03003631_g1), angiotensin II AT1 receptor (Mm01166161_m1), human STAT1 (Hs01014001_m1), mouse STAT1 (Mm01257276_g1), MMP-2 (Mm00439506_m1), and MMP-9 (Mm00600164_g1) were assayed using quantitative RT-PCR utilizing Taq-man Gene Expression Assays (Applied Biosystems, Foster City, CA). Briefly, aortic tissues were homogenized using TRIzol reagent (Invitrogen, Carlsbad, CA). mRNA was reverse transcribed and the resultant cDNA was amplified by Taq Polymerase (Promega, Madison, WI). Gene specific assays were performed and all data were normalized and analyzed using Applied Biosystems 7500 operating software. Final data are presented as expression of indicated molecules relative to expression of internal control probe sets as outlined in the systems instructions for use (Applied Biosystems).

Protein Immunoassay

Aortic protein was extracted using Cell Lytic-M (Sigma) lysis buffer. Total aortic protein was determined with the bicinchoninic acid (BCA) protein assay (Pierce, Rockford, IL). Human aortic samples were assayed for STAT1 using immunoblot assay. Briefly, protein extracts (20 ug/lane) were subjected to electrophoresis on a 10% Tris-glycine gel (Invitrogen), transferred to a nitrocellulose membrane, and blocked in 5% milk protein. Membranes were then incubated with antibodies for either STAT1 (1:2000), tyrosine(701)-phosphorylated STAT1 (1:1000) and serine(727)-phosphorylated STAT1 (1:1000) (Cell Signaling Technology, Beverly, MA) followed by incubation with horseradish peroxidase-conjugated goat anti-rabbit IgG secondary antibody (1:5000) and detection using ECL™ Westernblotting detection kit (Amersham Bioscience, Piscataway, NJ). Membranes were stripped and reprobed with an antibody to β -actin (Cell Signaling Technology). Membranes were exposed to Amersham Hyperfilm ECL (GE Healthcare). Films were scanned using an Epson Perfection 3200 Scanner (Epson America, Long Beach, CA) and band density was analyzed using Image J software (National Institute of Health, Bethesda, MD). Mouse total STAT1 and active STAT1 were assayed using a commercially available transcription factor assay (Human/Mouse Active STAT1 p91, R&D Systems, Minneapolis, MN). The active STAT1 assay is a transcription factor assay that uses a biotinylated double stranded oligonucleotide containing a consensus STAT1 binding site to capture and measure activated STAT1 (both tyrosine- and serine-phosphorylated forms).

Substrate gelatin zymography

Protein was isolated from the aqueous phase of TRIzol extraction and quantitated using the BCA protein assay. Semi quantitative MMP activity and distribution from harvested aortic protein extracts was determined by gelatin zymography as previously described¹². Briefly, after electrophoretic protein separation on precast 10% sodium dodecyl sulfate (SDS)-polyacrylamide gels containing 1mg/ml of gelatin (Novex, San Diego, CA), proteins were renatured in 2.7% Triton X-100 for 30 minutes and the gels subsequently incubated for 36 hours at 37°C in 50 mM Tris-HCl, 5 mM CaCl₂, and 0.2% Brij35. Following staining with Coomassie blue R-250 and destaining overnight with 10% acetic acid, gelatinase activity became evident by clear bands against a dark blue background. The relative molecular weight of each band was determined by comparison of the bands against MMP-2 (72 kDa) and MMP-9 (92 kDa) standards (Oncogene Research Products, Boston, MA). MMP activity was measured by standard densitometry techniques as described above.

Histologic and Immunohistochemical analysis

Aortic samples, at the time of harvest, were placed in 10% buffered formalin for 24 hours, followed by reagent alcohol 70% volume/volume for subsequent permanent section after paraffin embedding. Following deparaffinization, aortic sections were stained with hematoxylin and eosin. In addition, to further assess collagen distribution, samples were stained with Brillmeyer's trichrome stain. Following deparaffinization, samples were placed in hematoxylin for 40 seconds, followed by 0.2% (weight/volume) acid fuchsin for 1 minute. This was followed by a 3-hour incubation at room temperature in 0.5% aniline blue, 2% Orange G, and 1% phosphomolybdic acid in 100% ethanol. Movats stain was performed on deparaffinized aortic sections. Samples were placed in 1% Alician blue for 20 minutes, washed with water, and placed in alkaline alcohol at 56° C for 10 minutes. This was followed by serial exposure to the following solutions: Orcein-Verhoeff solution, Woodstain Scarlet-Acid Fuchsin solution, 0.5% acetic acid, 5% phosphotungstic acid, 100% ethyl alcohol, alcoholic saffron, and ultimately xylene.

For immunohistochemistry, tissue sections were deparaffinized and dehydrated through graded xylene and ethanol. For antigen retrieval, slides were incubated in the microwave for 20 minutes in 0.01 mol/L of citrate buffer, pH 6 (Fisher Scientific). To block endogenous peroxidase, the

slides were incubated in 3% H₂O₂ for 10 minutes at room temperature. Nonspecific binding was blocked by incubation with 5% normal goat serum for 30 minutes at room temperature. Incubation was then performed with 1:50 rabbit polyclonal to STAT1 (phosphoY701) (Abcam Inc, Cambridge, MA) and STAT1(phosphoS727) (Abcam). After rinsing in PBS-0.1% Tween 20, slides were incubated in anti-rabbit biotinylated secondary antibody (1:4000 dilution, Vector Laboratories, Burlingame, CA) for 30 minutes followed by incubation with Vectastain ABC Reagent (Vector Laboratories) for 30 minutes at room temperature. Immunoreactive cells were then visualized by the addition of diaminobenzidine (DAB, Vector Laboratories) and counterstained with hematoxylin.

Cholesterol, LDL, and LDL levels

Blood was collected from mice at the time of sacrifice and plasma isolated. Plasma samples were diluted 2:1 with a solution containing 500 mmol/L MgCl₂ and 10g/L dextran sulfate. After precipitation at room temperature for 10 minutes, the reaction mixture was centrifuged at 1500 g for 30 minutes at 4°C, and the supernatant was collected for determination of high density lipoprotein (HDL). The precipitate was re-suspended in 75 uL of D-PBS for determination of vLDL and LDL. Total cholesterol was determined by assaying 10 uL of plasma directly. ThermoTrace Cholesterol Reagent was added to the samples and allowed to sit for 15 minutes at room temperature. Spectrophotometrical measurements were made at 500 nm. Final values were obtained by plotting the optical density of the unknown samples on standard curves with cholesterol standards.

Statistical Analysis

Data were analyzed using non-paired T-test and analysis of variance. Significance was set at P<0.05. Analysis was performed using JMP 6.0.3 (SAS Institute Inc., Cary, NC). Results are expressed as mean ± standard error of the mean.

Results

Aortic aneurysm tissue was sampled from a cohort that was older (mean age 75.7±2.8 years) and had more men (80% men) than from whom non-aneurysmal tissue was sampled (mean age 37.6±5.7 years, and 60% men). STAT1 mRNA levels were 1.87-fold greater in AAA tissue compared to non-aneurysmal controls (P<0.05). In aneurysmal tissue, a 72% increase in total STAT1 protein (P<0.01) was observed (Fig. 1), while there was no increase in the fraction of STAT1 in the tyrosine- or serine-phosphorylated forms. When normalized to total protein, there was a trend toward elevated tyrosine-phosphorylated STAT1, but this did not reach statistical significance.

To gain further insight into STAT1 alterations during aortic aneurysm formation, STAT1 expression was evaluated during the process of experimental aortic aneurysm formation in the angiotensin II-infusion model of aneurysm formation. Aneurysm formation occurred in 0%, 12.5%, 50%, and 87.5% of apolipoprotein E null mice infused with angiotensin II for 0, 7, 14, and 28 days, respectively (n=8/time point). During this time period, there was a trend towards decreased total STAT1 protein levels over the first 14 days, but a significant increase in the fraction of STAT1 in the active form (P<0.05, Fig. 2). While there were changes in STAT1 protein levels and STAT1 activation, there were no temporal changes in STAT1 mRNA during Ang II infusion or when compared to baseline levels. As has been previously described, histologic evaluation of the aorta at this time point demonstrates the presence of an aortic dissection (Fig. 3)¹³. Immunohistochemical analysis for tyrosine-phosphorylated STAT1 demonstrates its presence in the inflammatory cells infiltrating the false lumen of the aortic dissection, but its presence is void from the regions adjacent to the true lumen (Fig. 3). Similar

staining with serine-phosphorylated STAT1 did not reveal any serine-phosphorylated staining at baseline or during the course of Ang II infusion.

Aortic aneurysm formation did not occur in STAT1 null mice infused with Ang II, but they did occur in ApoE/STAT1 null mice with 100% of the mice developing aortic aneurysm by 3 days of angiotensin II infusion. By 28 days of angiotensin II infusion, aortic aneurysms were larger in the apoE/STAT1 null mice compared to the apoE null mice (2.7 ± 0.4 mm v. 1.9 ± 0.1 mm, $P<0.05$) (Fig. 4). In addition, all of the aneurysms that occurred in the apoE/STAT1 null mice were of the type IV morphology, whereas this occurred in only 12.5% of the apoE null mice, which were predominantly the type III morphology (75%) (Fig. 4). In fact, in apoE/STAT1 null mice, aneurysm typically extended from the left subclavian artery to the aortic bifurcation. In addition, aortic rupture occurred more frequently in apoE/STAT1 null mice, occurring in 53% of apoE/STAT1 null mice infused with angiotensin II for longer than 3 days, and 81% of these mice infused longer than 5 days. Aortic rupture occurred in only 20% of apoE null mice. In addition, aortic rupture occurred earlier in apoE/STAT1 null mice (4.0 ± 0.5 days) compared to apoE null mice (9.2 ± 0.8 days, $P<0.05$). Gender proved to be protective against aneurysm formation, as neither female ApoE null mice nor ApoE/STAT1 double null mice formed aneurysm in response to 28 days of Ang II infusion (Fig. 4). Baseline systolic blood pressure did not differ significantly between apoE/STAT1 null mice and apoE null mice, and both groups responded with a similar increase in blood pressure in response to Ang II infusion (13 ± 3 mm Hg increase and 14 ± 6 mm Hg increase, respectively).

Baseline histologic evaluation of the aortic walls from apoE/STAT1 null and apoE null mice demonstrated no difference in the aortic wall architecture (Fig. 5). In addition, baseline expression of MMP-2 and MMP-9, based on aortic wall mRNA levels and aortic wall homogenate gelatin zymography, did not differ between the two strains of mice (Fig. 6). When evaluated after 28 days of Ang II infusion, total MMP-2 and MMP-9 levels, assessed by gelatin zymography, were 1.9-fold and 2.7-fold (respectively) higher than baseline levels in ApoE null mice, 1.8-fold and 2.9-fold higher than baseline levels in ApoE/STAT1 double null mice (Fig. 6), but only 0.9-fold and 1.1-fold different than baseline in STAT1 null mice. Furthermore, relative angiotensin II type I receptor mRNA expression did not differ significantly between the apoE $-/-$ mice and ApoE/STAT1 $-/-$ mice (1.0 ± 0.5 v. 0.6 ± 0.5 , respectively, $P=0.9$). Total cholesterol levels, however, were greater in the apoE/STAT1 null mice (333 ± 59 mg/dL) compared to apoE null mice (250 ± 48 mg/dL, $P<0.05$) (Fig. 6). The HDL and LDL fractions, however, did not differ significantly between the two groups.

Discussion

The aim of this study was to evaluate the potential role of STAT1 in aortic aneurysm formation. There is limited information regarding the role of STAT proteins in human AAA formation. The only previously available information was the result of gene expression profiling of aortic aneurysm tissue which demonstrated STAT1 mRNA was upregulated in human aortic aneurysms compared to non-aneurysm controls¹⁴. Our human data correlate with these findings and further demonstrate alterations in STAT1 protein production and activation. The human results from our analysis, however, need to be evaluated with caution. The patient population from which aortic tissue was procured was younger and had a higher percentage of women compared to those with aneurysmal disease. Because of this, we are not able to determine if the differences in STAT1 expression and activation are only due to the presence of an aneurysm, or if other factors are at play. We are not able to control for medications, other co-morbidities, or the presence of any significant atherosclerosis, all of which may alter the expression and activation of STAT1.

These confounding variables, however, are controlled for in the animal model. In Ang II infusion mouse model, while there is no increased STAT1 mRNA or total protein, STAT1 activation precedes aneurysmal degeneration. It does, however, appear to temporally be associated with the histologic presence of the aortic dissection. In addition, it appears that STAT1 may have a protective effect on the development of aortic dissection and subsequent aneurysmal degeneration as depletion of STAT1 is associated with earlier aneurysm formation, larger and more extensive aneurysmal degeneration, and a higher rate of aortic rupture. The current model depends on the infusion of Ang II in a hypercholesterolemic mouse. It differs from other mouse models of aneurysm formation in that it does not depend on the direct application of either Ca^{++} -chloride or porcine pancreatic elastase to the aorta^{1, 15}. It differs from these models, however, in that the aneurysm that forms is more consistent with the degeneration of an acute aortic dissection that develops in response to Ang II infusion. We are unable to determine from our observations whether the aortic ruptures that occur are due to profound accelerated aneurysmal degeneration or secondary to an acutely weakened aortic wall from the aortic dissection.

The mechanism by which these pathologies occur are not clear from the current information. The difference observed between the apoE/STAT1 null mice and STAT1 null mice may have multiple etiologies. The findings are independent of the hypertensive effects of Ang II infusion. There are equivalent systolic blood pressures in the ApoE $-/-$ and ApoE/STAT1 $-/-$ mice, and both strains respond equally with regard to elevation of systolic blood pressure with Ang II infusion. It is clear that the apoE/STAT1 mice have a more significant hypercholesterolemia, and this difference can be accentuated when these mice are placed on a high cholesterol diet⁹. We have yet to test whether ApoE/STAT1 $-/-$ mice, placed on a hypercholesterol diet, have altered rates of aneurysm formation. We have determined, however, that C57Bl/6J mice, placed on a variety of high cholesterol diets, have no alteration in aneurysm formation in response to Ang II infusion (data not shown). Interestingly, despite the higher total cholesterol levels, the loss of STAT1 was associated with diminished area of aortic atherosclerotic lesion formation⁹. These findings further support the hypothesis that aortic aneurysm pathogenesis is a process that occurs independent of atherosclerosis. We have previously demonstrated that hypercholesterolemic mice (apoE null mice) have significantly elevated AT1 receptor expression compared with normal-cholesterolemic controls¹¹. This may explain the increased responsiveness of hypercholesterolemic mice to Ang II infusion with aortic aneurysm formation^{16, 17}. It does not, however, explain the difference between a apoE/STAT1 null mice and apoE null mice as baseline aortic AT1 receptor expression did not differ between these two strains.

The influence of STAT1 on the development of more severe hypercholesterolemia is not known. STAT1, however, is one of the down-stream effectors of interferon- γ (IFN γ). IFN γ is known to promote a variety of pro-atherogenic effects through multiple mechanisms. In fact, evaluation of ApoE $-/-$ mice crossed with IFN γ receptor $-/-$ mice display a reduction in atherosclerotic lesion size and lipid accumulation¹⁸. In addition, alterations in lipid metabolism were noted in these mice as well, and a significant increase in distinct population of lipoprotein particles that are rich in apoA-IV, phospholipid, and free cholesterol. The mechanisms leading to these effects, however, are not known. IFN γ has been implicated in aortic aneurysm formation. Xiong et al. demonstrated that targeted deletion of IFN γ altered MMP expression and ameliorated aneurysm formation in a Ca^{++} -chloride model of aneurysm formation¹⁹. Alternatively, however, Libby and colleagues demonstrate that deletion of IFN γ led to increased expression of MMP-2 and MMP-9 and more severe aneurysm formation, in an alternate murine model of aortic aneurysm formation²⁰. These latter findings are more consistent with the observations in our current study. It may be, however, that the disparity observed in the effects of IFN γ are due to the differences in the model of aneurysm formation. Aside from Xiong's data, there is a growing body of work that demonstrates that loss of

IFN γ or STAT1 (a downstream mediator of IFN γ) is associated with decreased atherosclerotic lesions and with more accentuated aneurysm formation. These data further support the hypothesis that aneurysm formation is a process that occurs independent of the development of atherosclerosis. It may be, however, that the effects of the loss of STAT1 do not directly mirror those of IFN γ deletion as STAT1 is not the only downstream mediator of IFN γ signaling, nor is IFN γ the only promoter of STAT1 activation.

An alternate possibility is that the deletion of STAT1 has altered the baseline structural composition of the aorta. We did not, however, observe alterations in aortic wall collagen or elastin composition between the apoE/STAT1 null and apoE null strains. These observations were only made on non-specific histologic evaluations, and more specific analysis of collagen, elastin, and other aortic structural components is necessary. It has previously been demonstrated, however, that the loss of STAT1 is associated with a more severe fibroproliferative response in a mouse model of lung fibrosis²¹. This response was associated with an increase in total lung collagen content and enhanced fibroblast proliferation. Interestingly, the loss of STAT1 in this model was associated with increased activation of STAT3, which has been associated with IL-6 signaling, cell proliferation, and MMP-2 expression. The loss of STAT1 alone, however, is not sufficient to explain our findings in the apoE/STAT1 null mice as STAT1 null mice (apoE competent) did not form aneurysms in response to Ang II infusion.

In addition to altering the baseline composition of the aortic wall, the loss of STAT1 may be associated with altered expression of enzymes capable of degrading the aortic wall. The STAT1 pathway has been implicated in the expression of MMPs. Lentivirus infection of neural tissue promotes MMP-2 and MMP-9 expression and STAT1 activation²². Treatment of these neural cells with fludarabine, a pharmacologic STAT1 inhibitor, blocked the increased MMP-2 expression, but not MMP-9. Conversely, in STAT1 null fibrosarcoma tumor cells placed in an *in vivo* model of tumor growth, MMP-2 and MMP-9 expression could be suppressed by the reconstitution of STAT1²³. The results of these two studies demonstrate that in different cell lines, a specific STAT may have a different effect on the expression of a target protein (ie. in neural cells MMP2 production was STAT1-dependent, while in fibrosarcoma cells MMP-2 production was inhibited by STAT1). The baseline expression of MMP-2 and MMP-9 were not different between apoE/STAT1 null mice and apoE null mice. In addition, in both groups of mice the changes in MMP levels in response to Ang II infusion were similar between these two groups. Furthermore, STAT1 mice, which did not form aneurysms, did not have alterations in aortic MMP-2 or MMP-9 levels, assessed by gelatin zymography. This may suggest that alterations in STAT1 do not lead to alterations in MMP expression, at least in response to Ang II infusion. Ang II, however, is known to cause a rapid, yet transient, increase in tyrosine-phosphorylated STAT1^{24, 25}, and Ang II is known to induce expression of MMP-2 and MMP-9^{26, 27}. In addition, Ang II-dependent STAT1 activation and MMP expression are temporally associated²⁸. Our *in vivo* evaluation, however, has many variables that cannot be controlled for. Further evaluation *in vitro*, are warranted in order to better define the mechanisms involved in STAT-regulated MMP expression.

This current study again highlights the findings that female gender is protective against the development of aortic aneurysm formation. None of the apoE/STAT1 null or apoE null mice developed aneurysmal degeneration of the aorta with Ang II infusion. Low rates of aneurysm formation in this model have been previously described^{29, 30}. These findings are not unique to this mouse model of aneurysm formation, but have been described in alternate AAA mouse models³¹. Clearly more intensive investigations are necessary to determine why female gender is protective against aneurysm formation, but is beyond the scope of this study.

In conclusion, STAT1 appears to play an important role in aortic wall homeostasis and appears to be protective against the development of aortic dissection and aortic aneurysm degeneration. Further evaluations of the mechanisms that STAT1 may be affecting that contribute to this protective role are necessary and underway. A better understanding of the mechanisms contributing to aortic aneurysm formation is necessary in order to develop pharmacotherapies to aid in the treatment of this complex disease process. In addition, the apoE/STAT 1 null mouse may provide an excellent model with which to study alterations that occur during acute aortic dissection.

References

1. Davis V, Persidskaia R, Baca-Regen L, Itah Y, Nagase H, Persidsky Y, et al. Matrix metalloproteinase-2 production and its binding to the matrix are increased in abdominal aortic aneurysms. *Arterioscler Thromb Vasc Biol* 1998;18:1625–1633. [PubMed: 9763536]
2. Pyo R, Lee J, Shipley J, Curci J, Mao D, Ziporin S, et al. Targeted gene disruption of matrix metalloproteinase-9 (gelatinase B) suppresses development of experimental abdominal aortic aneurysms. *J Clin Invest* 2000;105:1641–1649. [PubMed: 10841523]
3. Thompson R, Parks W. Role of matrix metalloproteinases in abdominal aortic aneurysms. *Ann NY Acad Sci* 1996;800:157–174. [PubMed: 8958991]
4. Miyake T, Aoki M, Masaki H, Kawasaki T, Oishi M, Kataoka K, et al. Regression of abdominal aortic aneurysm by simultaneous inhibition of nuclear factor kB and ets in a rabbit model. *Circ Res* 2007;101:1175–1184. [PubMed: 17885220]
5. Nakashima H, Aoki M, Miyake T, Kawasaki T, Iwai M, Jo N, et al. Inhibition of experimental abdominal aortic aneurysm in the rat by use of decoy oligonucleotides suppressing activity of nuclear factor kB and ets transcription factors. *Circulation* 2004;109:132–138. [PubMed: 14662712]
6. Levy D, Darnell J Jr. STATs: Transcriptional control and biological impact. *Nature Rev* 2002;3:651–662.
7. Ihle J. The Stat family in cytokine signaling. *Curr Opin Cell Biol* 2001;13:211–217. [PubMed: 11248555]
8. Haura E, Turkson J, Jove R. Mechanisms of disease: insights into the emerging role of signal transducers and activators of transcription in cancer. *Nat Oncol* 2005;2:315–324.
9. Agrawal S, Febbraio M, Podrez E, Cathcart M, Stark G, Chisolm G. Signal transducer and activator of transcription 1 is required for optimal foam cell formation and atherosclerotic lesion development. *Circulation* 2007;115:2939–2947. [PubMed: 17533179]
10. Daugherty A, Manning M, Cassis L. Antagonism of AT2 receptors augments angiotensin II-induced abdominal aortic aneurysms and atherosclerosis. *Br J Pharmacol* 2001;134:865–870. [PubMed: 11606327]
11. Eagleton M, Ballard N, Lynch E, Srivastava S, Upchurch G, Stanely J. Early increased MT1-MMP expression and late MMP-2 and MMP-9 activity during angiotensin II induced aneurysm formation. *J Surg Res* 2006;135:345–351. [PubMed: 16716358]
12. Knipp B, Ailawadi G, Ford J, Peterson D, Eagleton M, Roelofs K, et al. Increased MMP-9 expression and activity by aortic smooth muscle cells after nitric oxide synthase inhibition is associated with increased nuclear factor-KB and activator protein-1 activity. *J Surg Res* 2004;116:70–80. [PubMed: 14732351]
13. Saraff K, Babamusta F, Cassis LA, Daugherty A. Aortic dissection precedes formation of aneurysms and atherosclerosis in angiotensin II-infused, apolipoprotein E-deficient mice. *Arterioscler Thromb Vasc Biol* 2003;23:1621–1626. [PubMed: 12855482]
14. Absi T, Sundt T III, Tung W, Moon M, Lee J, Damiano R, et al. Altered patterns of gene expression distinguishing ascending aortic aneurysms from abdominal aortic aneurysms: Complementary DNA expression profiling in molecular characterization of aortic disease. *J Thor Cardiovasc Surg* 2003;126:344–357.
15. Thompson R, Holmes D, Mertens R, Liao S, Botney M, Mecham R, et al. Production and localization of 92-kilodalton gelatinase in abdominal aortic aneurysms. *J Clin Invest* 1995;96:318–326. [PubMed: 7615801]

16. Daugherty A, Manning M, Cassis L. Angiotensin II promotes atherosclerotic lesions and aneurysms in apolipoprotein E-deficient mice. *J Clin Invest* 2000;105:1605–1612. [PubMed: 10841519]
17. Daugherty A, Cassis L. Chronic angiotensin II infusion promotes atherogenesis in low density lipoprotein receptor $-/-$ mice. *Ann NY Acad Sci* 1999;892:108–118. [PubMed: 10842656]
18. Gupta S, Pablo A, Jiang X, Wang N, Tall A, Schindler C. IFN-gamma potentiates atherosclerosis in ApoE-knockout mice. *J Clin Invest* 1997;99:2752–2761. [PubMed: 9169506]
19. Xiong W, Zhao Y, Prall A, Greiner T, Baxter B. Key roles of CD4+ T cells and interferon gamma in the development of abdominal aortic aneurysms in a murine model. *J Immunol* 2009;2004:2607–2612.
20. Shimizu K, Shichiri M, Libby P, Lee R, Mitchell R. Th2-predominant inflammation and blockade of IFN gamma signaling induce aneurysm in allografted aortas. *J Clin Invest* 2004;114:168–171. [PubMed: 15254583]
21. Walters D, Antao-Menezes A, Ingram J, Rice A, Nyska A, Tani Y, et al. Susceptibility of signal transducer and activator of transcription-1-deficient mice to pulmonary fibrogenesis. *Am J Pathol* 2005;167:1221–1229. [PubMed: 16251407]
22. Johnston J, Jiang Y, van Marle G, Mayne M, Ni W, Holden J, et al. Lentivirus infection in the brain induces matrix metalloproteinase expression: role of envelope diversity. *J Virol* 2000;74:7211–7220. [PubMed: 10906175]
23. Huang S, Bucana C, Van Arsdall M, Fidler I. Stat1 negatively regulates angiogenesis, tumorigenicity and metastasis of tumor cells. *Oncogene* 2002;21:2504–2512. [PubMed: 11971185]
24. Hernandez-Vargas P, Lopez-Franco O, Sanjuan G, Ruperez M, Ortiz-Munoz G, Suzuki Y, et al. Suppressors of cytokine signaling regulate angiotensin II-activated Janus Kinase-Signal Transducers and Activators of Transcription pathway in renal cells. *J Am Soc Nephrol* 2005;16:1673–1683. [PubMed: 15829701]
25. Banes-Berceli A, Shaw S, Ma G, Brands M, Eaton D, Stern D, et al. Effect of simvastatin on high glucose- and angiotensin II-induced activation of the JAK/STAT pathway in mesangial cells. *Am J Physiol Renal Physiol* 2006;291:F116–F121. [PubMed: 16449352]
26. Luchtefeld M, Grote K, Grothuse C, Bley S, Bandlow N, Selle T, et al. Angiotensin II induces MMP-2 in a p47phox-dependent manner. *Biochem Biophys Res Comm* 2005;328:183–188. [PubMed: 15670768]
27. Rouet-Benzineb P, Gontero B, Dreyfus P, Lafuma C. Angiotensin II induces nuclear factor-KB activation in cultured neonatal rat cardiomyocytes through protein kinase C signaling pathway. *J Mol Cell Cardiol* 2000;32:1767–1778. [PubMed: 11013121]
28. Wang T-L, Yang Y, Chang H, Hung C. Angiotensin II signals mechanical stretch-induced cardiac matrix metalloproteinase expression via JAK-STAT pathway. *J Mol Cell Cardiol* 2004;37:785–794. [PubMed: 15350851]
29. Manning MW, Cassis LA, Huang J, Szilvassy SJ, Daugherty A. Abdominal aortic aneurysms: fresh insights from a novel animal model of the disease. *Vasc Med* 2002;7:45–54. [PubMed: 12083734]
30. Martin-McNulty B, Tham D, daCunha V, Ho J, Wilson D, Rutledge J, et al. 17B-estradiol attenuates development of angiotensin II induced abdominal aortic aneurysm in apolipoprotein E deficient mice. *Arterioscler Thromb Vasc Biol* 2003;23:1627–1632. [PubMed: 12855485]
31. Ailawadi G, Eliason J, Roelofs K, Sinha I, Hannawa K, Kaldjian E, et al. Gender differences in experimental aortic aneurysm formation. *Arterioscler Thromb Vasc Biol* 2004;24:2116–2122. [PubMed: 15331435]

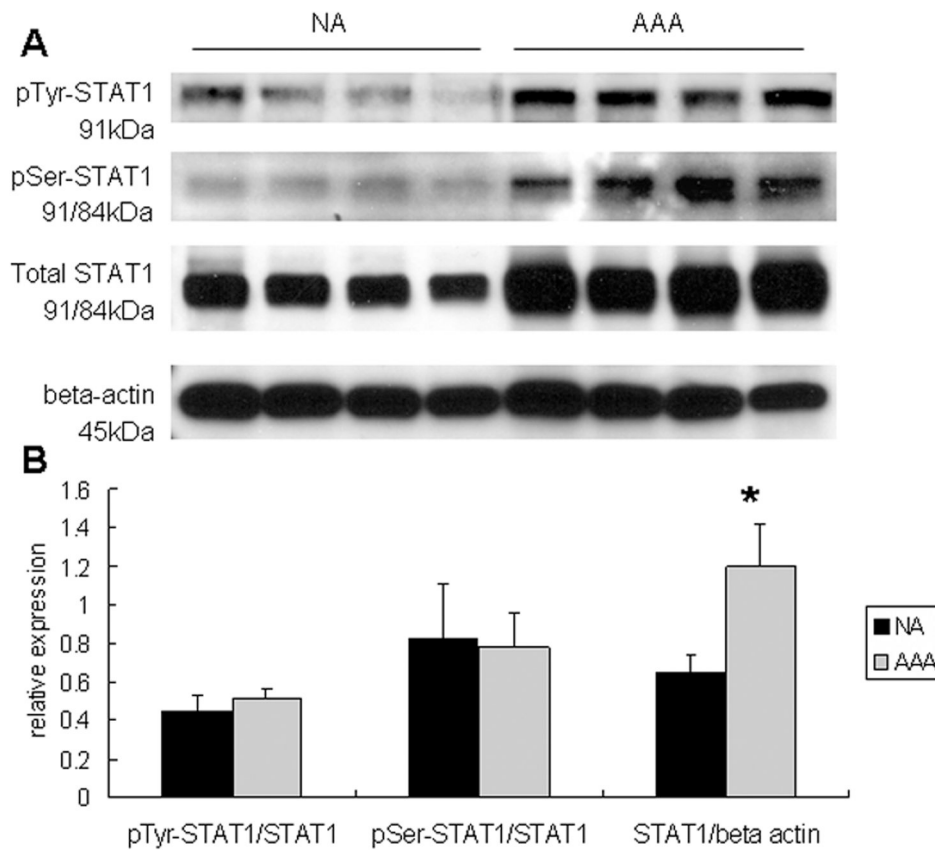


Figure 1.

(A) Representative immunoblots assessing tyrosine-, serine-, and total STAT1 from human aortic homogenates in those with abdominal aortic aneurysms (AAA) and those without aneurysms (NA). β -actin was also assayed in these samples. (B) Graphic demonstration of the fraction of STAT1 in the tyrosine- and serine-phosphorylated form. While there were no changes in the fraction of STAT1 in the different phosphorylated forms, there was a significant increase in total STAT1 protein from those with aneurysms (AAA) compared to those without (NA, $P < 0.05$).

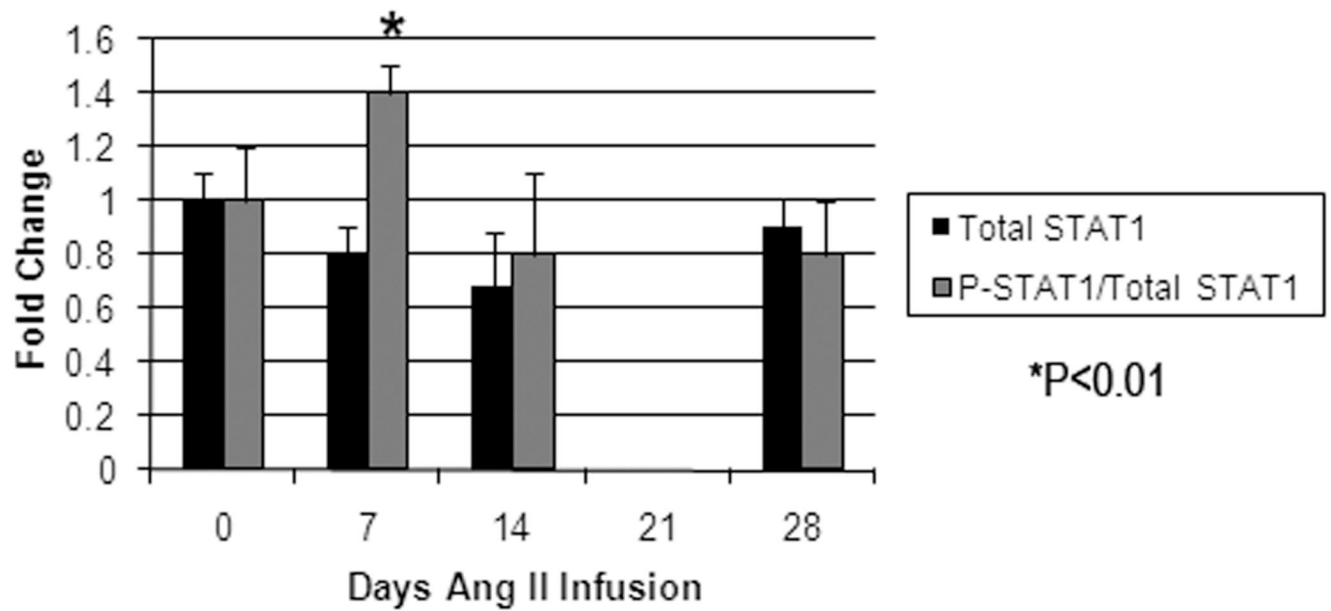


Figure 2.

Graphic presentation of temporal changes in aortic total STAT1 protein (black bars) and activated STAT1 protein (grey bars) and STAT1 mRNA from mice undergoing Ang II infusion (N=8/time point). Changes are normalized to baseline aortic levels. While there is a trend in a decrease in total STAT1 during the first two weeks of Ang II infusion, this did not reach statistical significance. There is, however, a significant increase in the fraction of STAT1 in the active form (both serine- and tyrosine-phosphorylated STAT1), peaking at 7 days of Ang II infusion (P<0.05).

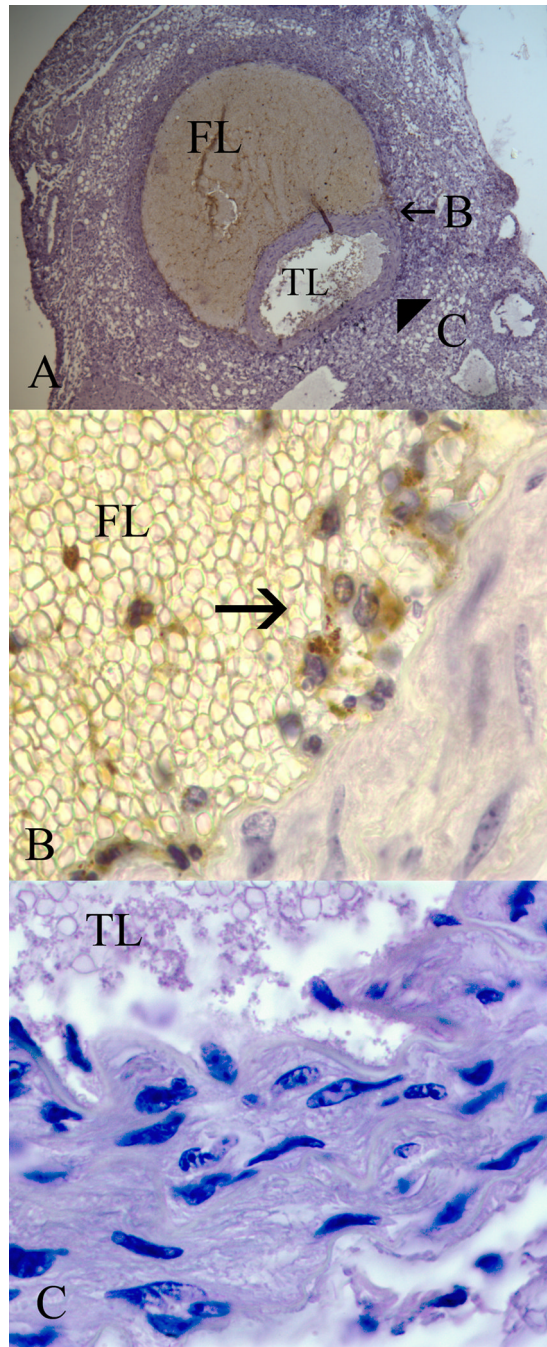


Figure 3. Representative immunohistochemical analysis of an apolipoprotein E null mouse aorta harvested at 7 days of Ang II infusion. **(A)** At 7 days there is evidence of an aortic dissection with a false lumen (FL) and patent true lumen (TL) (20x magnification). Immunohistochemical staining for tyrosine-phosphorylated STAT1 was performed, and regions of the aorta bordering the false lumen (B) and the true lumen (C) were evaluated under higher magnification (100x). **(B)** Inflammatory cells infiltrating the false lumen stain positively (arrow) for tyrosine-phosphorylated STAT1, but no positive staining is observed along the true lumen border **(C)**.

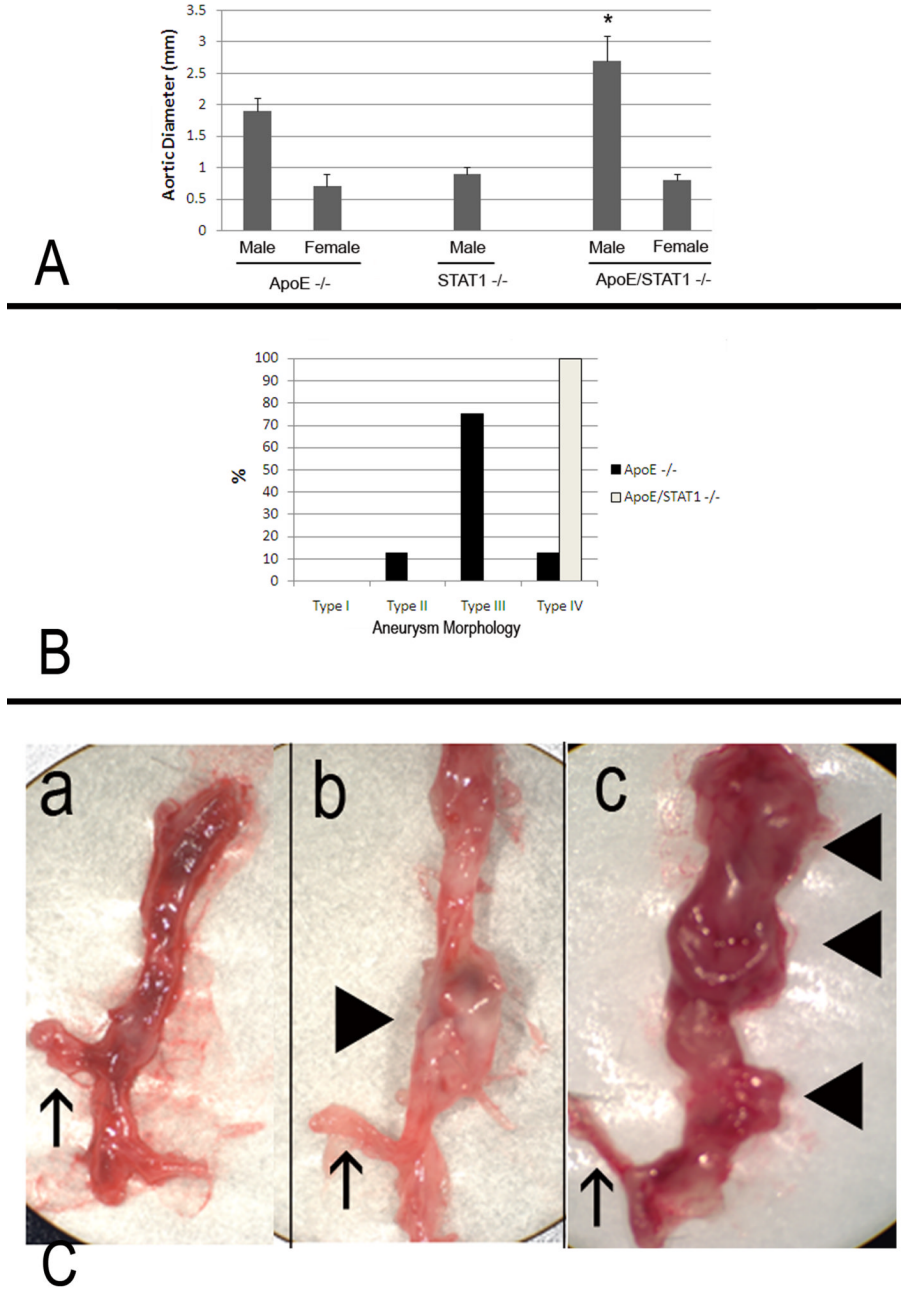


Figure 4. (A) Aortic diameters from male and female ApoE^{-/-}, STAT1^{-/-}, and ApoE/STAT1^{-/-} mice after 28 days of Ang II infusion. There were no significant aortic enlargements observed in STAT1^{-/-} male mice, nor in any of the female mice strains after 28 days of Ang II infusion. Aortic enlargement was observed in male ApoE^{-/-} and male ApoE/STAT1^{-/-} mice, and were larger in the ApoE/STAT1^{-/-} mice compared to the ApoE^{-/-} mice (P<0.05). (B) Graphic representation of aortic aneurysm morphology identified in ApoE^{-/-} male mice (black bars) and ApoE/STAT1^{-/-} male mice. All ApoE/STAT1 null mice developed the type IV phenotype. (C) Examples of aortas resected from (a) an ApoE^{-/-} mouse that did not undergo Ang II infusion, (b) an ApoE^{-/-} mouse that developed a type II morphology

aneurysm, and **(c)** an ApoE/STAT1 $-/-$ mouse that developed a type IV morphology aneurysm. The upward pointing arrows in all three instances denote the location of the right renal artery, while the block triangles point to locations of aneurysmal degeneration (only **b** and **c**)

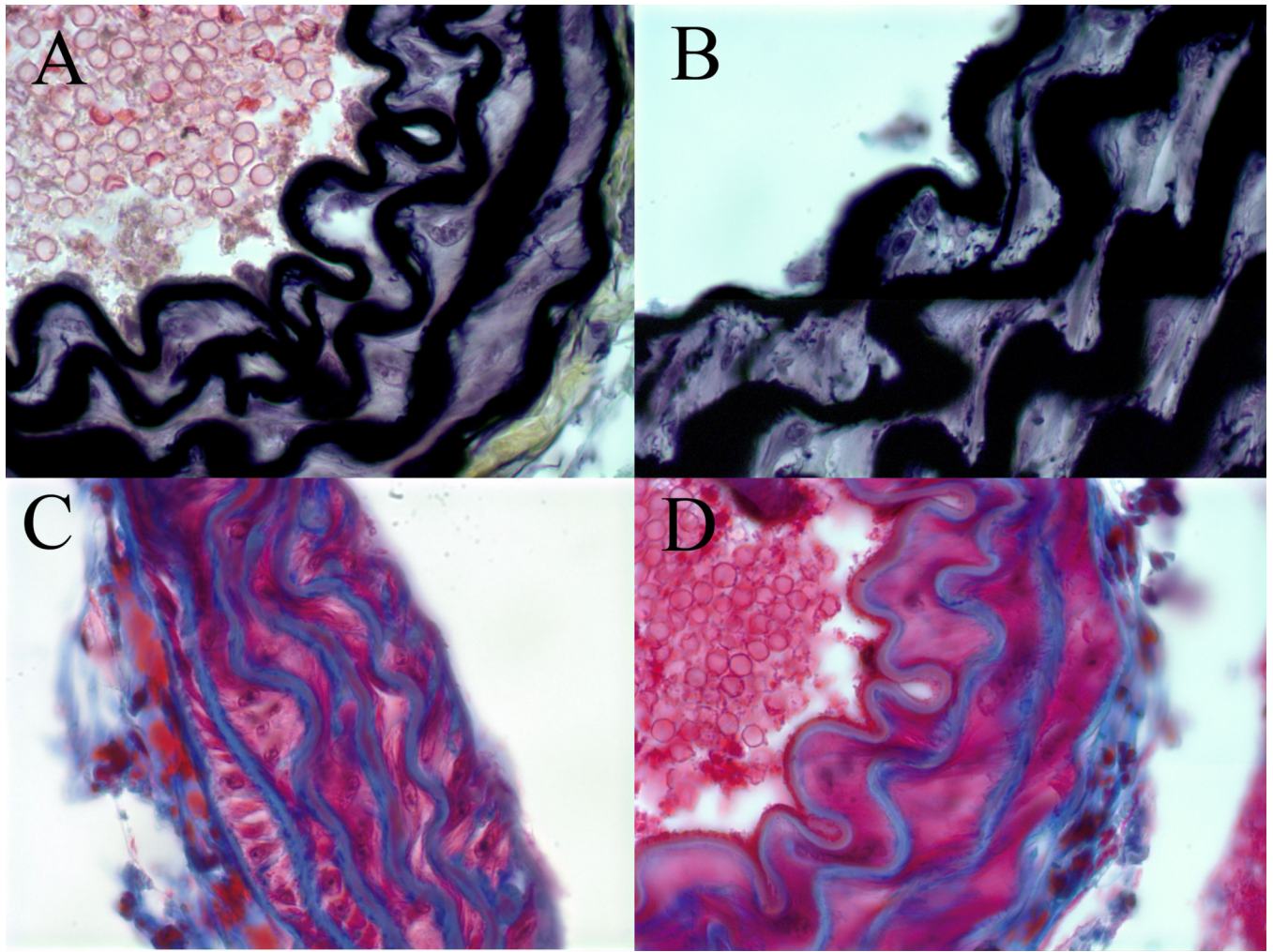
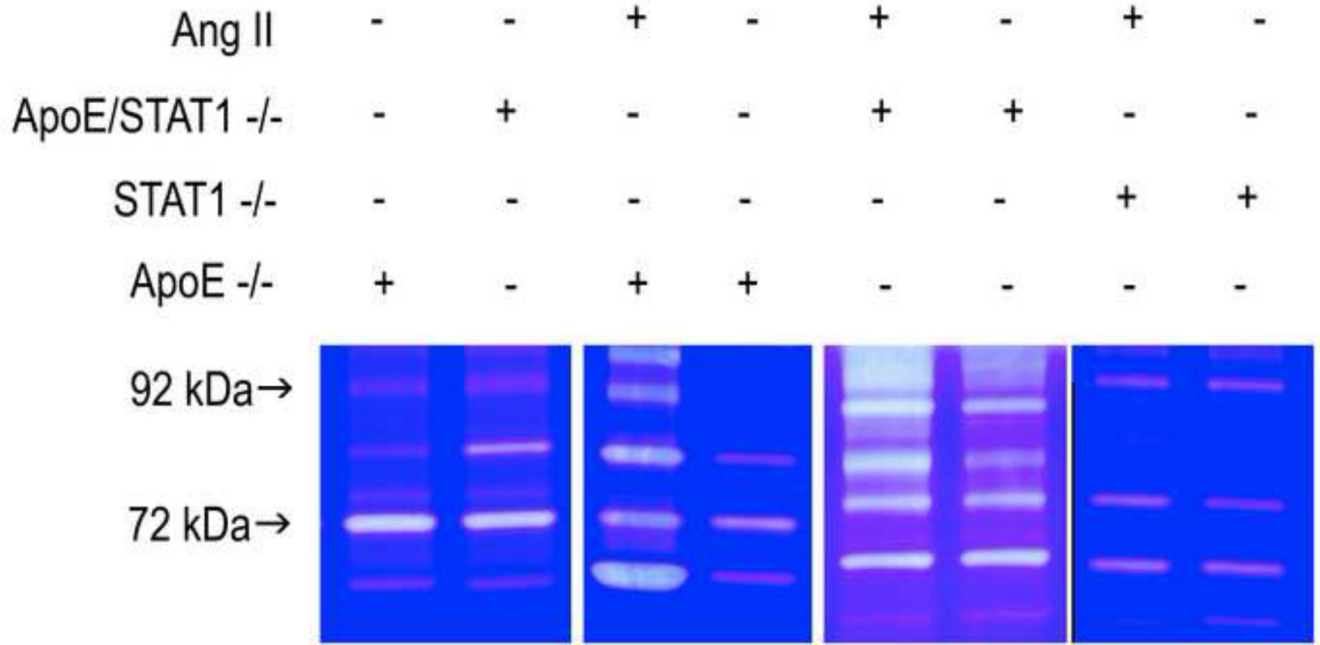
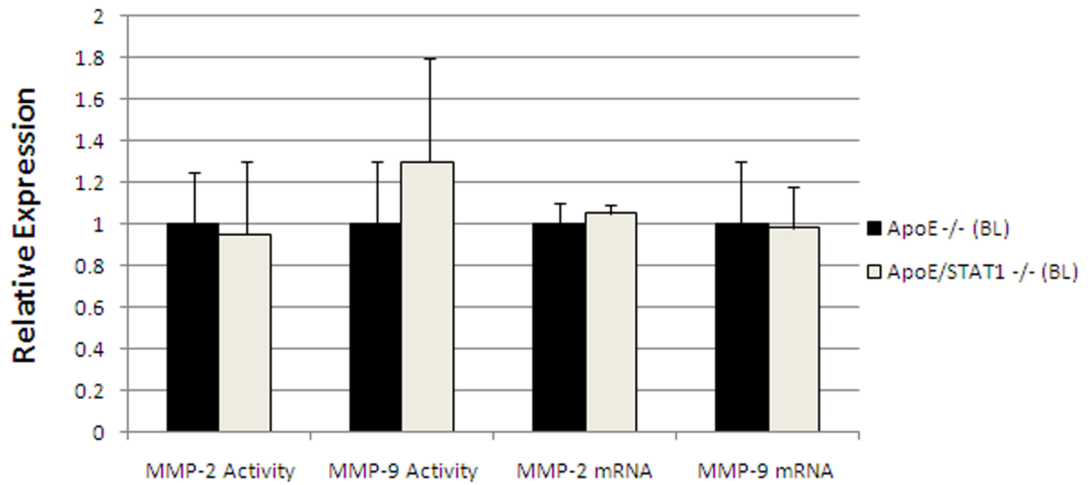


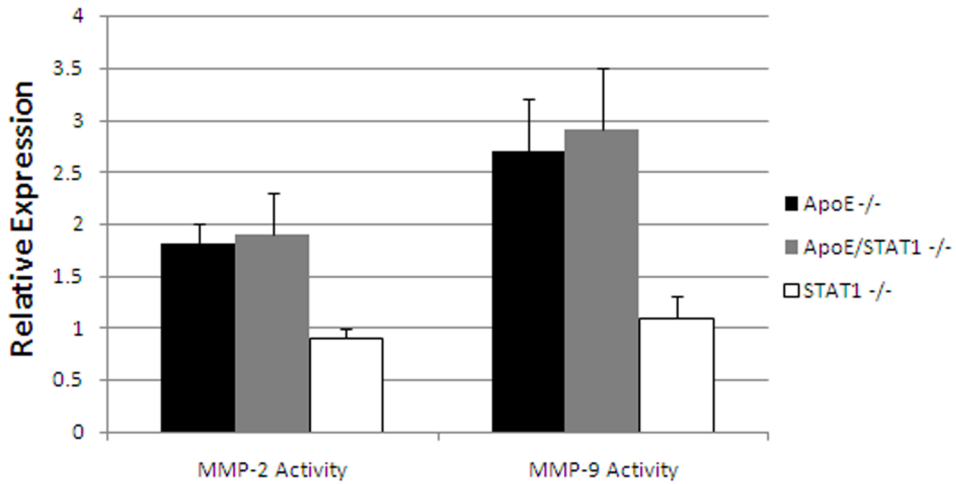
Figure 5. Representative sections of histologic analysis of elastin (**A, B**) content with Movat stain, and collagen content (**B, D**) with trichrome stain from the aortic walls of apoE/STAT1 null mice (**A, C**) and apoE null mice (**B, D**) (100x). No differences in elastic lamellae, elastin deposition, or collagen deposition are seen at baseline between these two mouse strains.



A



B



C

Figure 6.

(A) Representative gelatin zymograms from aortic homogenates from ApoE^{-/-}, STAT1^{-/-}, and ApoE/STAT1^{-/-} mice at baseline or following 28 days of Ang II infusion. The 92 kDa protein corresponds to pro-MMP-9 and the 72 kDa protein corresponds to pro-MMP-2. (B) Graphic representation of total MMP-2 and MMP-9 expression in ApoE^{-/-} (black bars) and ApoE/STAT1^{-/-} (grey bars) mice at baseline assessed by gelatin zymography and RT-PCR (N=5 mice/strain). Results are expressed relative to expression in ApoE^{-/-} mice. There is no significant difference in MMP activity or mRNA levels at baseline in these strains. (C) Graphic representation MMP-2 and MMP-9 activity (assessed by gelatin zymography) from aortic homogenates obtained from ApoE^{-/-} (black bars), ApoE/STAT1^{-/-} (grey bars), and STAT1^{-/-}

-/- (white bars) following 28 days of Ang II infusion (N=5 mice/strain). Results are expressed normalized to corresponding strains at baseline.

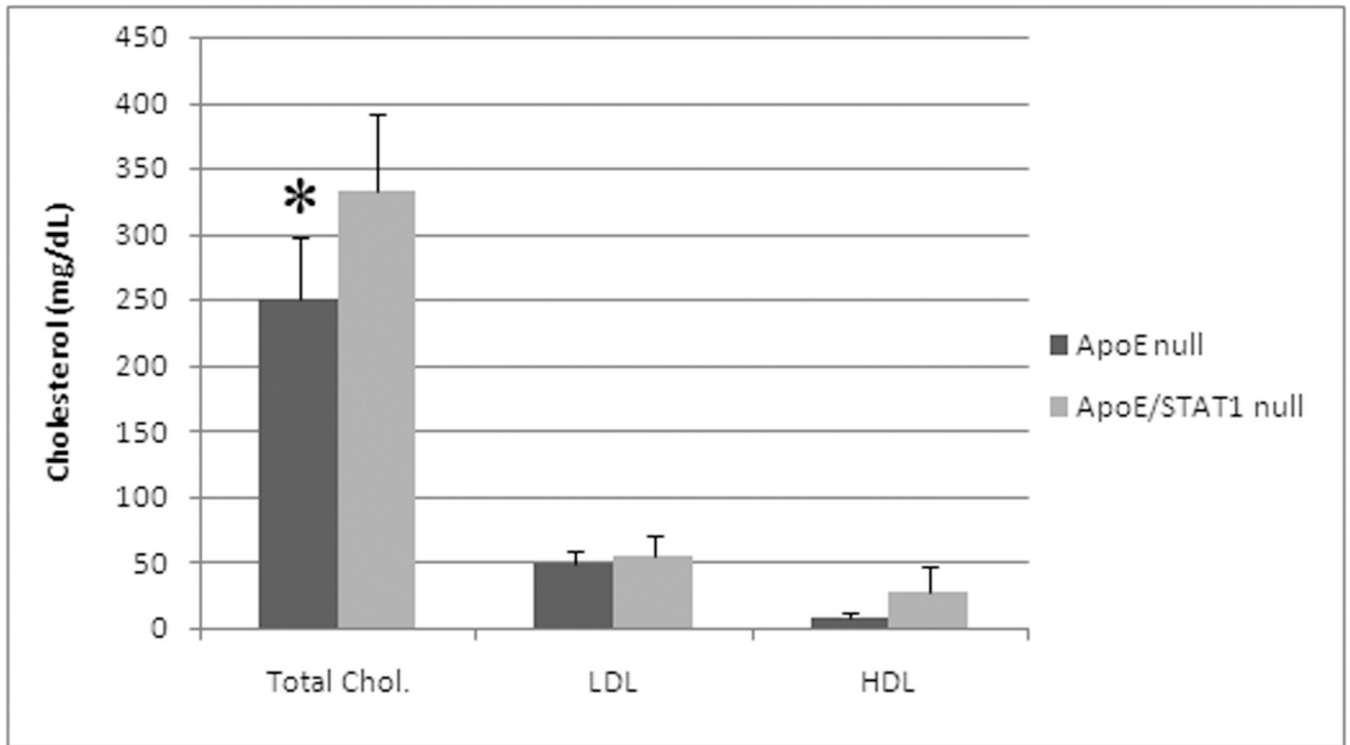


Figure 7. Graphic representation of total cholesterol, low density lipoprotein (LDL), and high density lipoprotein (HDL) from ApoE null mice and ApoE/STAT1 double null mice. Total cholesterol levels are higher in the ApoE/STAT1 double null mice compared with ApoE null mice ($P < 0.04$, *). HDL and LDL levels did not differ between these two mouse strains.